Compressive Strength of Cold-Formed Steel C-shape Columns with Slotted Holes

L. Xu

Y. Shi

S. Yang

Twenty-Second International Specialty Conference on Cold-Formed Steel Structures
St. Louis, Missouri, USA, November 5 & 6, 2014

Compressive Strength of Cold-formed Steel C-shape Columns with Slotted Holes

L. Xu[1], Y. Shi[2] and S. Yang[3]

Abstract

Presented in this paper is an experimental investigation on the effect of web holes on the strength of cold-formed steel (CFS) C-shape columns. A total of 18 CFS C-shape stub columns were tested without and with web holes. The column length and web height of C-shape section were 490 mm (19 in) and 150 mm (6 in), respectively; and the lengths of the holes investigated were 74 mm (3 in), 114 mm (4.5 in) and 130 mm (5 in) whereas the width of the holes remains as 38 mm (1.5 in). It is noted that for the strength determination of uniformly compressed stiffened elements with non-circular holes AISI-S100 requires the length of the holes not to exceed 114 mm (4.5 in). The test results obtained from this investigation showed that local buckling at the column ends combining with one distortional half-wave along the column length was the predominant failure mode. Results also indicate that the presence of web holes had negligible effect on the ultimate compressive strengths for the hole dimensions considered here. A numerical investigation based on elastic buckling analysis confirmed that the elastic local buckling load is not affected by the presence of the hole while the elastic distortional buckling load decreases slightly as the increase of the length of the hole. A comparison between results of the tests and the Direct Strength Method approach (DSM) for CFS columns with holes demonstrated that the DSM design equations are valid to evaluate the strength of CFS C-shape columns with web holes.

1. Introduction

Cold-formed steel (CFS) C-shape wall studs are commonly manufactured with holes to accommodate electrical, plumbing, and heating services' passages through walls and the installation of lateral bracing of the wall studs. The complexity associated with hole shape, size, and spacing has created a challenge

[1]Corresponding author: Professor, Department of Civil and Environmental Engineering, University of Waterloo, ON, Canada; E-mail: lxu@uwaterloo.ca
[2]Associate Professor, School of Civil Engineering, Chang'an University, Xi'an, China
[3]Research assistant, Department of Civil and Environmental Engineering, University of Waterloo, ON, Canada

on the determination of the compressive strength for CFS C-shape column with web holes. Current AISI-S100 (2012) stipulates that the strength determination based on the traditional effective-width based method for a stiffened element (e.g., the web of a C-section) with noncircular holes is limited to the width and length of a hole to be less than 63 mm (2.5 in) and 114 mm (4.5 in), respectively. Alternatively, the new approach developed by Moen and Schafer (2011) based on the Direct Strength Method (DSM) extends the limits on hole dimensions. The DSM based approach utilizes the finite strip analysis which accounts for the influence of holes on predicting the elastic buckling loads of a column, and then substitutes the obtained elastic buckling loads into a set of compressive strength prediction equations to determine the column strength. However, a limited number of tests were carried out to validate the accuracy and generality of the proposed DSM equations for columns with holes. This study aims to investigate the effect of the length of web holes on the behaviour CFS C-shape column. An experimental investigation was conducted for CFS C-shape stub columns with the length of web hole ranging from no holes to 130 mm (5 in). A numerical analysis of the effect of hole size on the elastic buckling shape and loads of stub column was also carried out. Finally, the test results were compared with the DSM based approach.

2. Experimental study

2.1. Stub column specimens

To study the effect of slotted web holes on the compressive strength of CFS C-shape columns, a total of 18 stub columns were tested, in which six specimens are solid section without a web hole and 12 specimens are with a pre-punched web slotted hole. The parameters investigated are the nominal thickness of steel (t) and the length of web hole (L_h). The nominal thicknesses of steel are 1.2 mm (47 mil) and 1.5 mm (59 mil), and the length of web hole ranges from no holes to 130 mm (5 in). The details of specimens and hole dimensions are shown in Figure 1 and Table 1, in which the first number of the designation denotes the length of web hole, the second and third digits represent the steel thickness, and the number of the specimen in a column group, respectively.

The material of the specimens was cold-formed galvanized steel. The length for all stub columns selected was 490 mm (19 in) to minimize the influence of global buckling and to ensure enough clear distance from the hole to the end of the specimen to avoid possible end effects. Both ends of the specimen were milled flat to ensure the full contact between the specimen and steel bearing plates. A slotted hole, located in the center of the web, has a constant width (d_h) of 38 mm (1.5 in). The three different lengths (L_h) of the holes as shown in

Table 1 were investigated. For each column group, three identical specimens were tested.

Mechanical properties for the C-shape columns were obtained from the tensile coupon tests as per the Chinese standard (GB/T228-2010 2009). Three tensile coupons were cut longitudinally from the web from a randomly selected C-shape CFS column for each thickness. The average material properties are listed in Table 2, where t is the steel thickness, f_y, f_u, E_s and v are steel yield stress, tensile strength, Young's modulus of elasticity and Possion's ratio, respectively.

Table 1 Stub column dimensions

Specimen No.	L (mm)	H (mm)	B (mm)	D (mm)	t (mm)	R (mm)	d_h (mm)	L_h (mm)
0-1.5-1 0-1.5-2 0-1.5-3	490	150	40	15	1.5	3.0	38	0
75-1.5-1 75-1.5-2 75-1.5-3	490	150	40	15	1.5	3.0	38	75
114-1.5-1 114-1.5-2 114-1.5-3	490	150	40	15	1.5	3.0	38	114
130-1.5-1 130-1.5-2 130-1.5-3	490	150	40	15	1.5	3.0	38	130
114-1.2-1 114-1.2-2 114-1.2-3	490	150	40	15	1.2	2.4	38	114
130-1.2-1 130-1.2-2 130-1.2-3	490	150	40	15	1.2	2.4	38	130

Table 2 Mechanical properties from tensile coupon tests

t (mm)	E_s (N/mm^2)	f_y (N/mm^2)	f_u (N/mm^2)	N
1.2	2.03×10^5	235	400	0.3
1.5	2.03×10^5	385	510	0.3

1 mm=1/25.4 in, 1 N/mm^2=1/6.895 ksi.

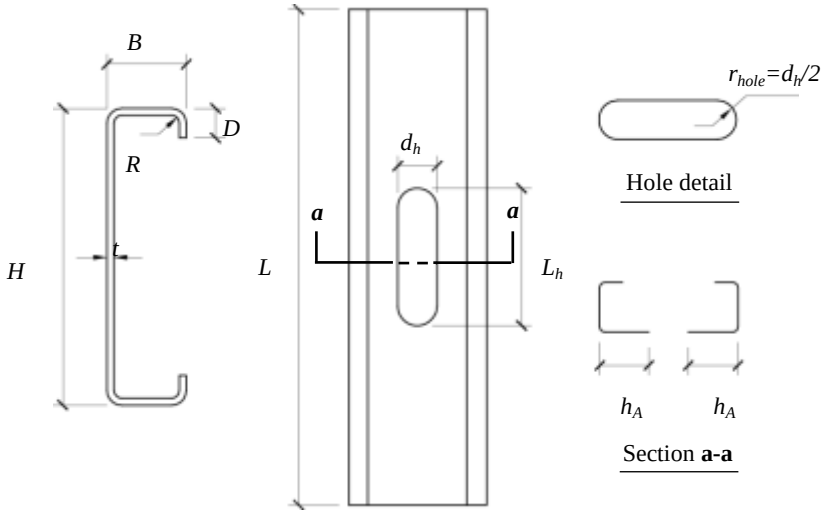

Figure 1 Specimen dimensions

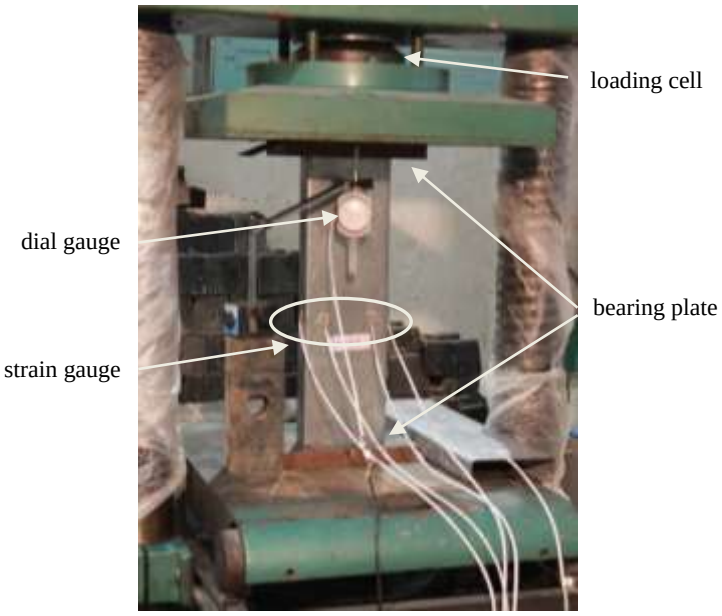

Figure 2 Experimental setup

2.2. Experimental setup

Shown in Figure 2 is the setup of the experimental investigation. The compressive tests were conducted on a hydraulic compressive test frame system with loading capacity of 2,000 kN (450,000 lb). The load was applied uniformly and concentrically to each column specimen through two loading bearing plates. The column cross section was restrained from lateral movement at ends only by the friction-bearing conditions. The axial deformation of each specimen was measured with a dial gauge, and the longitudinal strains were recorded by four uniaxial strain gauges placed at the mid height cross section as shown in Figure 2. The loading was applied with an increment of one-tenth of the estimated axial capacity of each specimen until the failure of the specimen. The smaller load increment was adopted when applied load approached to the axial capacity.

3. Elastic buckling analysis

A study on elastic buckling of the tested specimens was conducted to investigate the influence of the length of hole on the elastic buckling behaviour of the specimens (i.e., elastic buckling modes associated with elastic buckling loads).

3.1. Elastic buckling shape

The elastic buckling shapes of the stub columns were obtained from the buckling analysis using the finite element software ABAQUS (ABAQUS 2012). The specimens were modelled with 4-node shell elements (S4R) with global mesh dimension of a 5 mm (0.2 in). The material properties E_s, f_y and υ were taken as that shown in Table 2.

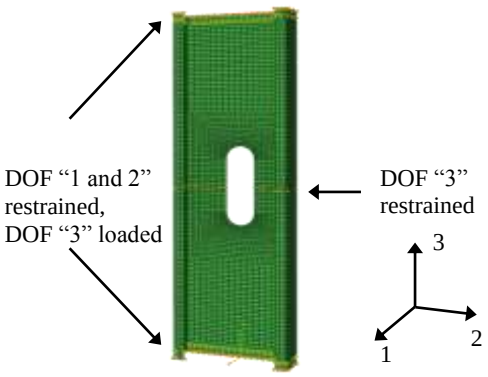

Figure 3 Load and boundary conditions in ABAQUS modelling

The boundary and loading conditions were modeled as warping free at the both ends and warping fixed at the mid length of the member (Figure 3), as described by Moen and Schafer (2006).

Shown in Figure 4 and 5 are the local and distortional buckling modes obtained from the buckling analysis for 1.5mm (59mil) specimens, respectively. The local and distortional buckling modes are identified according to the half-wavelengths presented in Table 3 based on the semi-analytical finite strip analysis using software CUFSM (CUFSM 2006). For a member with a hole, the local and distortional buckling modes are obtained from the second and third buckling modes, respectively, except the distortional mode for the member with a 130 mm (5 in) long hole is selected from the fourth buckling mode. For members without holes, buckling analysis results show local buckling mode governs and distortional buckling mode does not occur; local buckling mode is selected as the lowest buckling mode.

For local buckling mode, the mode shapes are similar to that shown in Figure 4 for all members. However, for members with web holes, the local web deformation at the hole location is apparently influenced by the length of the hole. For distortional mode, the member buckles with a combination of local and distortional buckling, and the number of local buckling half-waves changes from one to two when the hole length increases to 130 mm as shown in Figure 5. Although Figures 4 and 5 are based on the members with thickness of 1.5 mm, similar phenomena are also observed for members with steel thickness 1.2 mm.

Table 3 Local and distortional buckling half-wavelengths obtained from CUFSM

Specimens	Elastic buckling half-wavelength	
	Local buckling (mm)	Distortional buckling (mm)
0-1.2; 0-1.5	110	350

3.2. Elastic buckling loads

Due to relatively short length of the specimens, global buckling (i.e., flexural, torsional, or flexural-torsional buckling) does not occur; thus, only elastic buckling loads associated with local and distortional buckling modes (P_{crl} and P_{crd}) were investigated by finite strip analysis with software CUFSM (Schafer and Ádàny 2006).

For members without holes, the elastic buckling loads are obtained from the two local minimums of the elastic buckling curve (Li and Schafer 2010). For members with holes, the elastic buckling loads P_{crl} and P_{crd} can be determined

from software CUFSM with accounting for the influence of the hole (Moen and Schafer 2009).

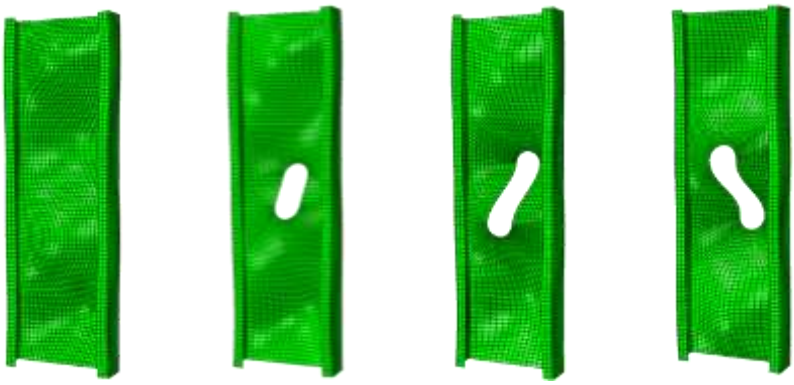

a) 0-1.5 b) 75-1.5 c) 114-1.5 d) 130-1.5

Figure 4 Local buckling mode shapes of 1.5 mm specimens

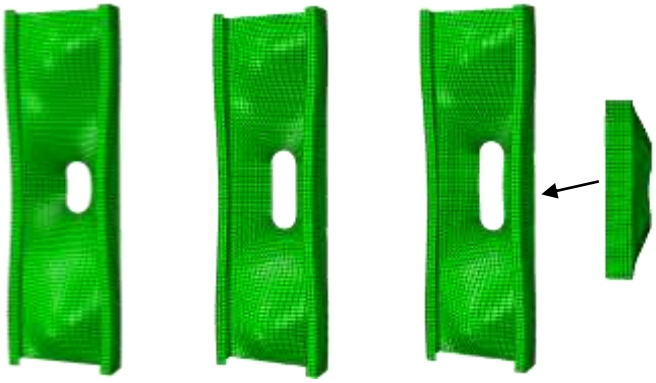

a) 75-1.5 b) 114-1.5 c) 130-1.5

Figure 5 Distortional buckling mode shapes of 1.5 mm specimens

The elastic buckling load ratios obtained from CUFSM corresponding to the local and distortional buckling modes at a hole width to out-to-out web depth (d_h/H) of 0.25 are plotted in Figure 6 as a function of unstiffened strip aspect ratio (L_h/h_A); where h_A is the unstiffened strip width adjacent to the hole in the web. In this investigation, h_A remains as a constant of 56 mm (2.2 in) for all stub columns with holes. Ratio L_h/h_A is an important parameter in the determination of the plate buckling coefficient for an unstiffened strip in compression in the

DSM approach (Moen and Schafer 2008b). $P_{y,g}$, P_{crl} and P_{crd} are member gross section yield strength, local and distortional buckling loads, respectively. It can be seen that because of the presence of the hole, with the variation of L_h/h_A ratio, the local buckling loads P_{crl} remains almost unchanged while P_{crd} alters.

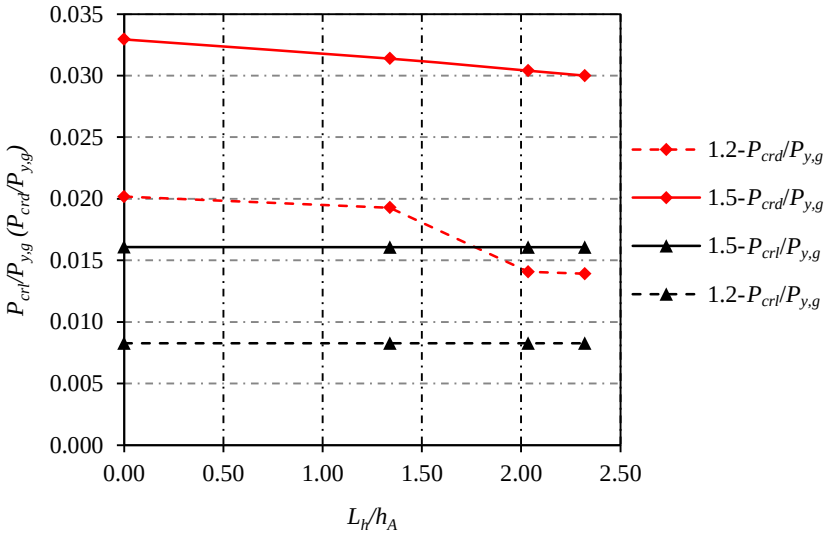

Figure 6 Influence of hole length on local and distortional buckling loads (d_h/H=0.25)

4. Experimental results

Shown in Figure 7 are the failure modes of the specimens. The typical failure mode observed was local buckling of the web near both column ends together with inward distortional buckling with only one half-wave located longitudinally between the two ends. For the specimens shown smooth half sine wave in web near the hole, larger out-of-plane deflection at the center of the web and more localized deformation in both flanges at the mid-height of the column were observed when compared to the specimens without the hole. This is primarily due to the presence of the web hole. The existence of the hole degrades the transverse plate stiffness of the web which deteriorates the rotation restraint provided by the web to the flange. Consequently, both the web and flange deformations around the hole are increased. Comparing to Figure 5, it can be seen that the typical failure modes of the specimens match well with the distortional buckling mode shapes predicted by the elastic buckling analysis. However, owing to the possible presences of initial geometrical imperfections

and minor misalignments in the specimens, local buckling concentrated in flanges and unstiffened strips adjacent to web holes were observed in a few specimens, such as the one on the right of Group 130-1.5.

a) Group 0-1.5 b) Group 75-1.5

c) Group 114-1.5 d) Group 130-1.5

e) Group 114-1.2 f) Group 130-1.2

Figure 7 Specimen failure modes

The typical load-displacement curve for each specimen group obtained from the tests are shown in Figure 8. The differences in the ultimate loads (P_{test}) among the three identical specimens for each group are found to be less than 7%. It can be seen from the figure that the length of web hole has little influence on the ultimate loads.

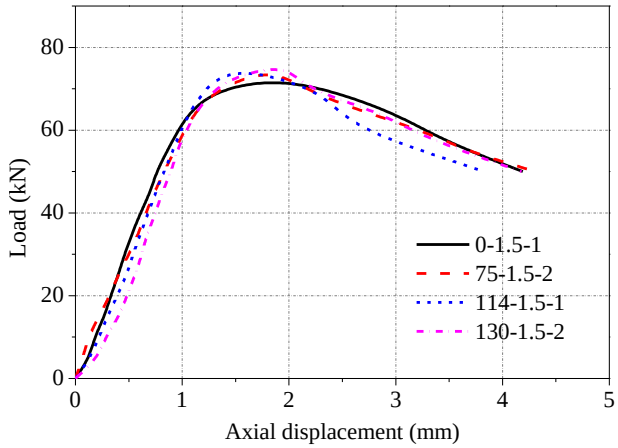

Figure 8 Load-displacement relationships

5. Comparison with DSM approach

The ultimate loads of 18 specimens obtained in this experiemental investigation are used to assess the accuracy of the DSM approach on predicting the strength of CFS columns with holes. According to the DSM approach, the nominal axial strength, P_n, is calculated as the minimum strength from the local, distortional, and global buckling, i.e., P_n=min (P_{nl}, P_{nd}, P_{ne}). The limit state strengths, P_{nl}, P_{nd}, and P_{ne}, are determined from equations (1)-(9) for members without hole (AISI-S100 2007), and equations (1)-(6) and (10-16) for members with holes (Schafer and Ádàny 2010).

(a) Flexural, torsional, or flexural-torsional buckling

$$\text{for } \lambda_c \le 1.5, \quad P_{ne} = \left(0.658^{\lambda_c^2}\right) P_y \tag{1}$$

$$\text{for } \lambda_c > 1.5, \quad P_{ne} = \left(\frac{0.877}{\lambda_c^2}\right) P_y \tag{2}$$

where

$$\lambda_c = \left(P_y / P_{cre}\right)^{0.5} \tag{3}$$

(b) Local buckling or local-global buckling interaction

The nominal axial strength, P_{nl}, is calculated as follows:

$$\lambda_l \le 0.776, \quad P_{nl} = P_{ne} \tag{4}$$

$$\text{for } \lambda_l > 0.776, \quad P_{nl} = \left[1 - 0.15\left(\frac{P_{crl}}{P_{ne}}\right)\right]^{0.4}\left(\frac{P_{crl}}{P_{ne}}\right)^{0.4} P_{ne} \tag{5}$$

where

$$\lambda_l = \left(P_{ne} / P_{crl}\right)^{0.5} \tag{6}$$

(c) Distortional buckling

For columns without hole,

$$\lambda_d \le 0.561, \quad P_{nd} = P_y \tag{7}$$

$$\text{for } \lambda_d > 0.561, \quad P_{nd} = \left[1 - 0.25\left(\frac{P_{crd}}{P_y}\right)\right]^{0.6}\left(\frac{P_{crd}}{P_y}\right)^{0.6} P_y \tag{8}$$

where

$$\lambda_d = \left(P_y / P_{crd}\right)^{0.5} \tag{9}$$

For columns with hole,

$$\text{for } \lambda_d < \lambda_{d1}, \quad P_{nd} = P_{ynet} \tag{10}$$

$$\text{for } \lambda_{d1} < \lambda_d \le \lambda_{d2}, \quad P_{nd} = P_{ynet} - \left(\frac{P_{ynet} - P_{d2}}{\lambda_{d2} - \lambda_{d1}}\right)(\lambda_d - \lambda_{d1}) \tag{11}$$

$$\text{for } \lambda_d > \lambda_{d2}, \quad P_{nd} = \left(1 - 0.25\left(\frac{P_{crd}}{P_y}\right)^{0.6}\right)\left(\frac{P_{crd}}{P_y}\right)^{0.6} P_y \tag{12}$$

where

$$\lambda_d = \left(P_y / P_{crd}\right)^{0.5} \tag{13}$$

$$\lambda_{d1} = 0.561\left(P_{ynet} / P_y\right) \tag{14}$$

$$\lambda_{d2} = 0.561\left\lfloor 14\left(P_{ynet} / P_y\right)^{0.4} - 13\right\rfloor \tag{15}$$

$$P_{d2} = \left(1 - 0.25\left(\frac{1}{\lambda_{d2}}\right)^{1.2}\right)\left(\frac{1}{\lambda_{d2}}\right)^{1.2} P_y \tag{16}$$

In the foregoing equations, λ_c, λ_l and λ_d are the slenderness ratios; P_y and P_{net} are the column squash loads associated with gross and net sections, respectively. P_{cre} is the global elastic buckling load; and P_{crl} and P_{crd} are the elastic local and distortional buckling loads calculated in the previous section, respectively.

Table 4 Comparison of test results with the DSM approach

Specimen No.	A_g (mm^2)	A_{net} (mm^2)	P_{test} (kN)	P_{ne} (kN)	P_{nl} (kN)	P_{nd} (kN)	P_n (kN)	P_n/P_{test} (kN)
0-1.5-1			76.0					1.06
0-1.5-2	374	317	73.0	131.40	71.52	80.64	71.52	1.02
0-1.5-3			74.0					1.03
75-1.5-1			70.0					0.98
75-1.5-2	374	317	75.0	131.34	71.50	78.80	71.50	1.05
75-1.5-3			74.0					1.03
114-1.5-1			75.0					1.05
114-1.5-2	374	317	76.0	131.26	71.47	77.60	71.47	1.06
114-1.5-3			73.0					1.02
130-1.5-1			73.0					1.02
130-1.5-2	374	317	76.0	131.23	71.46	77.10	71.46	1.06
130-1.5-3			78.0					1.09
114-1.2-1			42.0					1.07
114-1.2-2	299	254	40.0	66.48	39.43	41.09	39.43	1.01
114-1.2-3			40.0					1.01
130-1.2-1			43.0					1.09
130-1.2-2	299	254	43.0	66.46	39.43	40.87	39.43	1.09
130-1.2-3			43.0					1.09

Shown in Table 4 are the ultimate compressive strengths obtained from the tests and the strengths predicted by the DSM approach. It can be found that local buckling loads are always the lowest one for all the buckling limit states, which signifies all the specimens were governed by local buckling. The ratio of local and distortional buckling loads (P_{nl}/P_{nd}) ranges from 0.89 to 0.96. As the increase of length of hole, ratio P_{nl}/P_{nd} approaches to 1.0, representing the intensive interaction between local and distortional buckling. When ratio L_h/h_A =2.32, i.e., L_h=130 mm(5 in), ratio P_{nl}/P_{nd} approaches to 0.93 and 0.96 for specimens with thickness of 1.5 and 1.2 mm (49 and 57 mil), respectively;

which indicates sections with thinner thickness is more likely involved with the interaction of local and distortional buckling.

From Table 4, it also can be seen that the nominal strengths of the specimens with web holes evaluated by the DSM approach are in good agreement with those of tests. The nominal strengths P_n evaluated by DSM approach are slightly greater than the tested ultimate strengths P_{test} except one case. The differences between the two are less than 9%. Thus, it is concluded that DSM approach is accurate on determining the compressive strength of C-shape CFS members with non-circular holes for a length of hole up to 130 mm (5 in).

6. Conclusions

The effects of web holes on the failure mode and ultimate strength of CFS C-shape stub columns are investigated in this study. Conclusions obtained from this study are summarized as follows:

- Based on the experimental investigation on 18 stub column specimens with and without non-circular web holes, the observed typical failure mode is local buckling at the column ends combined with distortional buckling occurred at one distortional half-wave away from both column ends. Regarding to the ultimate strength of the columns, tested results show the presence of holes has negligible effect on the ultimate compressive strengths for the hole dimensions investigated in this study.

- The foregoing conclusion is also confirmed by the elastic buckling analysis of the specimens using finite element analysis software ABAQUS. The analysis further unveils the variation of length of hole may result in a change in buckling shape. The interaction of local and distortional buckling modes detected by the buckling analysis matches well with the typical failure modes observed from the tests. Although the local buckling load is not affected by the presence of a web hole, the distortional buckling load appears to decrease slightly as the increase the length of the hole.

- The comparison between the tested ultimate strengths and the strengths calculated based on the DSM approach demonstrates that the DSM approach provides accurate assessments on the compressive strength of C-shape CFS member with non-circular holes for the hole dimensions investigated in this study. In addition, the limitation on the length of holes to not exceed 114 mm (4.5 in) in AISI-S100 may be extended to 130 mm (5 in).

References

ABAQUS (2012). *ABAQUS/Standard Users Manual version 6.12*. ABAQUS, Inc., www.abaqus.com, Providence, RI.

GB/T228-2010. (2010). *Tensile Test Method for the Metal Materials at Room Temperature*. Standardization Administration of the People's Republic of China, Beijing.

Li, Z. and B. W. Schafer. "Application of the finite strip method in cold-formed steel member design." *Journal of Constructional Steel Research* 66, no. 8, 2010: 971-980.

Moen, C. D. and Schafer, B. W. (2008). "Experiments on cold-formed steel columns with holes." *Thin-Walled Structures* 46, no. 10, 2008: 1164-1182.

Moen, C. D. (2008). "Direct Strength Design of Cold-formed Steel Members with Perforations." PhD thesis, Johns Hopkins University.

Moen, C. D. and Schafer, B. W. (2009). "Elastic buckling of cold-formed steel columns and beams with holes." *Engineering Structures* 31, no. 12, 2009: 2812-2824.

Moen, C. D. and B. W. Schafer. (2011) "Direct strength method for design of cold-formed steel columns with holes." *Journal of Structural Engineering*, ASCE, 137, no. 5, 2011: 559-570.

AISI-S100. (2012). North American Specification for the Design of Cold-Formed Steel Structural Members, American Iron and Steel Institute. Washington, D.C.

Schafer, B. W., and S. Ádány. (2006). "Buckling analysis of cold-formed steel members using CUFSM: conventional and constrained finite strip methods." *Proceeding of 8th international specialty conference on cold-formed steel structures*, pp. 39-54, Oct. 26-27, 2006. Orlando, Florida